



## Quantitative assessment of fire and vegetation properties in historical simulations with fire-enabled vegetation models from the Fire Model Intercomparison Project

5 Stijn Hantson<sup>1,2</sup>, Douglas I. Kelley<sup>3</sup>, Almut Arneith<sup>1</sup>, Sandy P. Harrison<sup>4</sup>, Sally Archibald<sup>5</sup>,  
Dominique Bachelet<sup>6</sup>, Matthew Forrest<sup>7</sup>, Thomas Hickler<sup>7,8</sup>, Gitta Lasslop<sup>7</sup>, Fang Li<sup>9</sup>, Stephane  
Mangeon<sup>10,a</sup>, Joe R. Melton<sup>11</sup>, Lars Nieradzik<sup>12</sup>, Sam S. Rabin<sup>1</sup>, I. Colin Prentice<sup>13</sup>, Tim  
Sheehan<sup>6</sup>, Stephen Sitch<sup>14</sup>, Lina Teckentrup<sup>15,16</sup>, Apostolos Voulgarakis<sup>10</sup>, Chao Yue<sup>17</sup>.

10 <sup>1</sup> Karlsruhe Institute of Technology, Institute of Meteorology and Climate research, Atmospheric Environmental  
Research, Garmisch-Partenkirchen, Germany.

<sup>2</sup> Geospatial Data Solutions Center, University of California Irvine, CA 92697 Irvine, USA.

<sup>3</sup> Centre for Ecology and Hydrology, Wallingford OX10 8BB, UK.

<sup>4</sup> School of Archaeology, Geography and Environmental Sciences, University of Reading, Reading, UK.

15 <sup>5</sup> Centre for African Ecology, School of Animal, Plant and Environmental Sciences, University of the  
Witwatersrand, Private Bag X3, WITS, Johannesburg, 2050, South Africa.

<sup>6</sup> Biological and Ecological Engineering, Oregon State University, Corvallis, OR 97331, USA.

<sup>7</sup> Senckenberg Biodiversity and Climate Research Institute (BiK-F), Senckenberganlage 25,  
60325 Frankfurt am Main, Germany.

20 <sup>8</sup> Institute of Physical Geography, Goethe-University, Altenhöferallee 1, 60438 Frankfurt am Main, Germany.

<sup>9</sup> International Center for Climate and Environmental Sciences, Institute of Atmospheric Physics,  
Chinese Academy of Sciences, Beijing, China.

<sup>10</sup> Department of Physics, Imperial College London, London, UK.

<sup>11</sup> Climate Research Division, Environment and Climate Change Canada, Victoria, BC V8W 2Y2, Canada

25 <sup>12</sup> Institute for Physical Geography and Ecosystem Sciences, Lund University, 22362 Lund, Sweden.

<sup>13</sup> AXA Chair of Biosphere and Climate Impacts, Grand Challenges in Ecosystem and the Environment,  
Department of Life Sciences and Grantham Institute – Climate Change and the Environment, Imperial College  
London, Silwood Park Campus, Buckhurst Road, Ascot SL5 7PY, UK.

<sup>14</sup> College of Life and Environmental Sciences, University of Exeter, Exeter EX4 4RJ, UK.

30 <sup>15</sup> ARC Centre of Excellence for Climate Extremes, University of New South Wales, Sydney, NSW, Australia.

<sup>16</sup> Climate Change Research Center, University of New South Wales, Sydney, NSW 2052, Australia.

<sup>17</sup> Laboratoire des Sciences du Climat et de l'Environnement, LSCE/IPSL, CEA-CNRS-UVSQ, Université Paris-  
Saclay, 91198 Gif-sur-Yvette, France.

<sup>a</sup> now at: Data 61, CSIRO, Brisbane, Australia

35

*Correspondence to:* Stijn Hantson (hantson.stijn@gmail.com)



**Abstract.** Global fire-vegetation models are widely used to assess impacts of environmental change on fire regimes and the carbon cycle, and to infer relationships between climate, land use, and fire. However, differences in model structure and parameterizations, in both the vegetation and fire components of these models, could influence overall model performance, and to date there has been limited evaluation of how well different models represent various aspects of fire regimes. The Fire Model Intercomparison Project (FireMIP) is coordinating the evaluation of state-of-the-art global fire models, with the aim of improving projections of fire regime characteristic and fire impacts on ecosystems and human societies under the context of global environmental change. Here we perform a systematic evaluation of historical simulations made by nine FireMIP models in order to quantify their ability to reproduce a range of fire and vegetation benchmarks. The FireMIP models simulate a wide range in global annual total burnt area (39-536 Mha), and global annual fire carbon emission (0.91-4.75 Pg C a<sup>-1</sup>) for modern conditions (2002-2012), but most of the range in burnt area is within observational uncertainty (345-468 Mha). Benchmarking scores indicate that seven out of nine FireMIP models are able to represent the spatial pattern in burnt area. The models also reproduce the seasonality in burnt area reasonably well but struggle to simulate fire season length and are largely unable to represent inter-annual variations in burnt area. However, models that represent cropland fires see improved simulation of fire seasonality in the northern hemisphere. The three FireMIP models which explicitly simulate individual fires are able to reproduce the spatial pattern in number of fires, but fire sizes are too small in key regions and this results in an underestimation of burnt area. The correct representation of spatial and seasonal patterns in vegetation appears to correlate with a better representation of burnt area. While some FireMIP models are better at representing certain aspects of the fire regime, no model clearly outperforms all other models across the full range of variables assessed.

## 1 Introduction

Fire is a crucial ecological process that affects vegetation structure, biodiversity, and biogeochemical cycles in all vegetated ecosystems (Bond et al., 2005; Bowman et al., 2016) and has serious impacts on air quality, health, and economy (e.g. Bowman et al., 2009; Lelieveld et al., 2015; Archibald et al., 2013). In addition to naturally occurring wildland fires, fire is also used as a tool for pasture management and to remove crop residues. Because fire affects a large range of processes within the Earth system, modules which simulate burnt area and fire emissions are increasingly included in dynamic global vegetation models (DGVMs) and Earth System Models (ESMs) (Hantson et al., 2016; Kloster and Lasslop, 2017; Lasslop et al., 2019). However, the representation of both wildfires and anthropogenic fires varies greatly in global models. This arises due to the lack of a comprehensive understanding of how fire ignitions, spread, and suppression are affected by weather, vegetation, and human activities, as well as the relative scarcity of long-term, spatially resolved data on the drivers of fires and their interactions (Hantson et al., 2016). As a result, model projections of future fire are highly uncertain (Settele et al., 2014; Kloster and Lasslop, 2017). Since vegetation mortality – including fire-related death – is one determinant of carbon residence time in ecosystems (Allen et al., 2015), differences in the representation of fire in DGVMs or ESMs also contributes to the uncertainty in trajectories of future terrestrial carbon uptake (Ahlström et al., 2015; Friend et al., 2014; Arora & Melton, 2018). Improved projections of wildfires and anthropogenic fires, their impact on ecosystem properties, and their socio-economic impact will therefore support a wide range of global environmental change assessments, as well as the development of strategies for sustainable management of terrestrial resources.



Although individual fire-enabled DGVMs have been evaluated against observations, comparisons of model performance under modern-day conditions tend to focus on a limited number of fire-related variables or specific regions (e.g. French et al., 2011; Wu et al., 2015; Ward et al., 2016; Kloster and Lasslop, 2017). Such comparisons do not provide a systematic evaluation of whether different parameterizations or levels of model complexity provide a better representation of global fire regimes than others. Likewise, none of the Coupled Model Intercomparison Projects that have been initiated to support the IPCC process (CMIP: Taylor et al., 2012; Eyring et al., 2016) focuses on fire, even though several of the CMIP models simulate fire explicitly. The Fire Model Intercomparison Project (FireMIP) is a collaborative initiative to systematically evaluate state-of-the-art global fire models (Hantson et al., 2016; Rabin et al., 2017).

The FireMIP initiative draws on several different types of simulations, including a baseline historical simulation (1700-2013 CE) and sensitivity experiments to isolate the response of fire regimes to individual drivers, as well as simulations in which fire is deliberately excluded (Rabin et al., 2017). While the sensitivity and exclusion experiments provide valuable insights into model behaviour (Teckentrup et al., 2019; Li et al., 2019), the baseline historical simulation provides an opportunity to assess how well the models simulate modern conditions. Model-model differences could reflect differences in the treatment of fire, of ecosystem processes, or how fire interacts with other aspects of the land surface in an individual model. Evaluation of the baseline simulations needs therefore to include evaluation of ecosystem processes and diagnosis of interactions between simulated vegetation and fire.

Systematic model evaluation can also serve another purpose. The analysis of future climate and climate impacts is often based on results from climate and impact model ensembles (e.g. Kirtman et al., 2013; Collins et al., 2013; Warszawski et al. 2013) and these ensembles are also being used as a basis for impact assessments (e.g. Settele et al., 2014; Hoegh-Guldberg et al., 2019). However, there is increasing dissatisfaction with the idea of using the average behaviour of model ensembles without accounting for the fact that some models are less reliable than others (Giorgi and Mearns 2002; Knutti, 2010; Parker et al., 2013) and many have called for “the end of model democracy” (e.g. Held, 2005; Knutti, 2010). Although there is still considerable discussion about how to constrain models using observations, and then how to combine and possibly weight models depending on their overall performance or performance against a minimum set of specific criteria (e.g. Eyring et al., 2005; Tebaldi et al., 2005; Gleckler et al., 2008; Weigel et al., 2008; Santer et al., 2009; Parker, 2013; Abramowitz et al., 2019), it is clear that results from systematic evaluations are central to this process.

A number of papers have examined specific aspects of the FireMIP baseline simulations. Andela et al. (2017) showed that the FireMIP models do not reproduce the decrease in global burnt area over the past two decades inferred from analysis of version 4s of the Global Fire Emission Database (GFED4s) data product. In fact, four of the models show an increase in burnt area over the period 1997-2014. Although the remaining five models show a decrease, their mean decrease is only about one tenth of the observed rate ( $-0.13 \pm 0.56\% \text{ yr}^{-1}$ , compared to the observed trend of  $-1.09 \pm 0.61\% \text{ yr}^{-1}$ ). However, the observed global decline of burnt area derived from satellite data is strongly dominated by African savanna ecosystems, the spatial pattern of trends is very heterogeneous, and the satellite record is still very short, which raises issues about the robustness of these trends (Forkel et al., 2019b). Li et al. (2019) compared modelled and satellite-based fire emissions and concluded that most FireMIP models fall within the current range of observational uncertainty. Forkel et al. (2019a) compared the emergent relationships between burnt area and multiple potential drivers of fire behaviour, including human caused ones, as seen in observations and the FireMIP models. They show that, although all of the models capture the observed emergent relationships with climate variables, there are large differences in their ability to capture vegetation-related



relationships. This is underpinned by a regional study using the FireMIP models over China, which showed that there are large differences in simulated vegetation biomass, and hence in fuel loads, between the models (Song et al., 2019). These results make a focus on benchmarking both simulated fire and vegetation particularly pertinent. Forkel et al. (2019a) showed that some of the FireMIP models, specifically those that include a relatively strong fire suppression associated with human activities (Teckentrup et al., 2019), were able to reproduce the emergent relationship with human population density. However, the treatment of the anthropogenic influence on burnt area has been identified as a weakness in the FireMIP models (Andela et al., 2017; Teckentrup et al., 2019; Li et al., 2019; Forkel et al., 2019a), mainly due to a lack of process understanding.

In this paper, we focus on quantitative evaluation of model performance using the baseline historical simulation and a range of vegetation and fire observational datasets. We identify (i) common weaknesses of the current generation of global fire-vegetation models (ii) factors causing differences between the models, and (iii) priorities for future model development.

## 2 Methods

### 2.1 Model Simulations

The baseline FireMIP simulation is a transient experiment starting in 1700 CE and continuing to 2013 (see Rabin et al., 2017 for description of the protocol). Models were spun up until carbon stocks were in equilibrium for 1700 CE conditions (equilibrium was defined as <1% change over a 50 year time period for the slowest carbon pool in each grid cell) using land use and population density for 1700 CE, CO<sub>2</sub> concentration for 1750 CE, and recycling climate and lightning data from 1901-1920 CE. Although the experiment is fully transient after 1700 CE, annually varying values of all these forcings are not available until after 1900 CE. Climate, land use, population and lightning were regridded to the native grid of each model. Global fire-vegetation models ran with either dynamic or prescribed natural vegetation (Table 1), but all used observed time-evolving cropland and pasture (if simulated) distribution.

Nine coupled fire-vegetation models have performed the FireMIP baseline experiments. The models differ in complexity, representation of human impact and vegetation dynamics, and spatial and temporal resolution (Table 1). A detailed description of each model is given in Rabin et al. (2017). Most of the models ran simulations for the full period 1700-2013, but CLASS-CTEM, JULES-INFERNO, MC2 and CLM simulated 1861-2013, 1700-2012, 1902-2009 and 1850-2013 respectively. This slight deviation from the protocol does not affect the results presented here as we only analyse data for present-day period.

### 2.2) Model Evaluation and Benchmarking

Model performance was evaluated using site-based and remotely sensed global data sets of vegetation properties, fire occurrence and fire-related emissions (Figure 1; Figure S1). We used multiple datasets as targets for variables where they were available in order to take into account observational uncertainty. We used the GFED4 (Giglio et al., 2013), GFED4s (Randerson et al., 2012), MCD45 (Roy et al., 2008), FireCC4.0 (Alonso-Canas and Chuvieco, 2015) and FireCCI5.1 (Chuvieco et al., 2018) burnt area datasets; the Global Fire Assimilation System (GFAS) fire emissions (Kaiser et al., 2012); fire size and number from Hantson et al. (2015); site-level net primary productivity (NPP) and gross primary productivity (GPP) from Luyssaert et al. (2007), as well as NPP from the Ecosystem Model/Data Intercomparison (EMDI; Olson et al., 2001), from Michaletz et al. (2014) and upscaled



fluxnet GPP data (Jung et al., 2017; Tramontana et al., 2017); aboveground vegetation biomass from Carvalais et al. (2014) and Avitabile et al. (2016); and Leaf Area Index (LAI) from MODIS MCD15 (Myneni et al., 2002) and AVHRR (Claverie et al., 2016). A complete description of the reference data sets used for benchmarking is given in the Supplementary Information S1 and all datasets are plotted in Figure S1. For comparison and application of the benchmark metrics, all the target datasets and model outputs were resampled to a  $0.5^\circ$  grid. Although some models were run at a coarser resolution, the spatial resolution at which the benchmarking was performed had only a limited impact on the scores (Figure S2), which does not affect conclusions drawn here. Each model was compared to each reference dataset except in the few cases where the appropriate model output was not provided (e.g. LAI in ORCHIDEE, GPP in MC2). Only the models which incorporate the SPITFIRE fire module provided fire size and number results.

While we use multiple datasets to attempt to quantify observational uncertainty, this only addresses one area of observational uncertainty. Most observation-based datasets don't provide estimates of measurement error and uncertainty. As well, most datasets haven't been independently validated and could suffer from methodological issues affecting quality. Therefore, large uncertainties still remain for most variables, even well-established ones such as burnt area (e.g. Roteta et al., 2019). When uncertainties of datasets are known one can take this into account by weight the model scores less for the less trustworthy datasets (e.g. Collier et al. 2018). However, as the uncertainty of most reference datasets are currently unknown, we haven't attempted that here and instead treat each dataset equally. As model benchmarking techniques become more sophisticated it would be beneficial to better evaluate the datasets the models are compared against to ensure the models are being benchmarked appropriately.

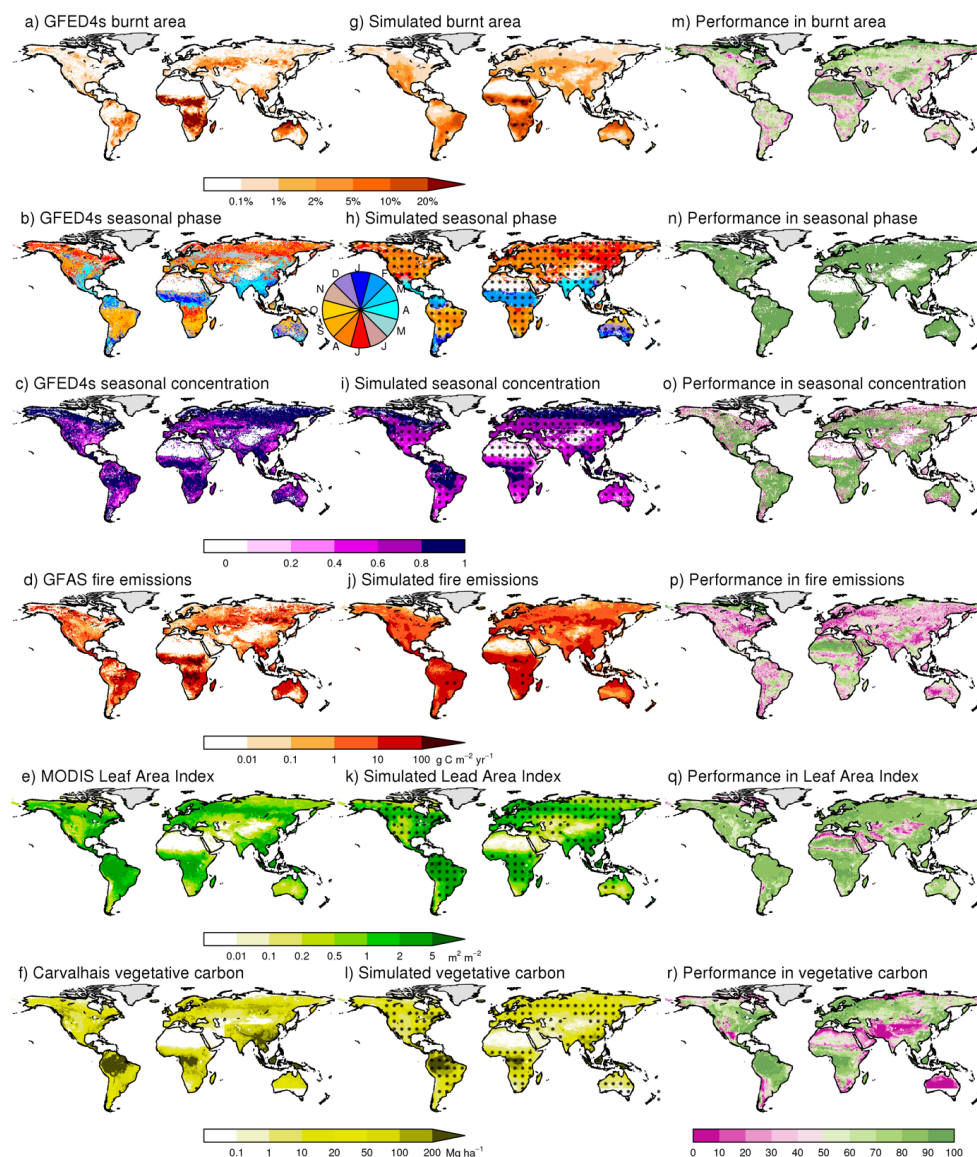
We use the normalised mean error (NME), which is the mean absolute difference between a simulated and observed variable normalised by the observational variance, to assess each model's ability to reproduce spatial patterns in annual average burnt area and the other variables that influence burnt area. We therefore removed the influence of biases in the mean and variance between model results and reference datasets (See Supplementary Information S2) because NME can be sensitive to the simulated magnitude and this furthermore limits the impact of observational uncertainties in the reference datasets.

Seasonality comparisons were conducted in two parts: seasonal concentration (roughly equivalent to the inverse of season length) and phase, or timing, of the season. We calculated a mean seasonal "vector" in a given observed location or simulated cell based on the monthly distribution of burnt area throughout the year. The concentration is the length of this vector compared to annual burnt area, and ranges between 0 when fire is equally spread throughout the year to 1 when all burning occurs in the same month. The phase is indicated by the direction of the vector. Observed and modelled concentrations were compared using NME, and phases compared using the Mean Phase Difference (MPD) metric (see Supplementary Information S2). Three models simulate or provided only annual burnt area (LPJ-GUESS-GlobFIRM, LPJ-GUESS-SIMFIRE-BLAZE, MC2) and thus the seasonality benchmarks could not be calculated for these models. We did not use FireCC4.0 to assess seasonality or interannual variability (IAV) in burnt area because it has a much shorter times series than the other burnt area products.

NME and MPD are both proportional to mean absolute errors, so the smaller the value the better the model performance. A score of 0 represents a perfect match to observations. NME has no upper bound, whereas MPD has a maximum value of 1 when all cells have a maximum phase mismatch of 6 months. Model scores are further interpreted by comparing to two null models (Kelley et al., 2013): the "mean" null model compares the mean value of the observations to the observations; and the "randomly-resampled" null model compares observations

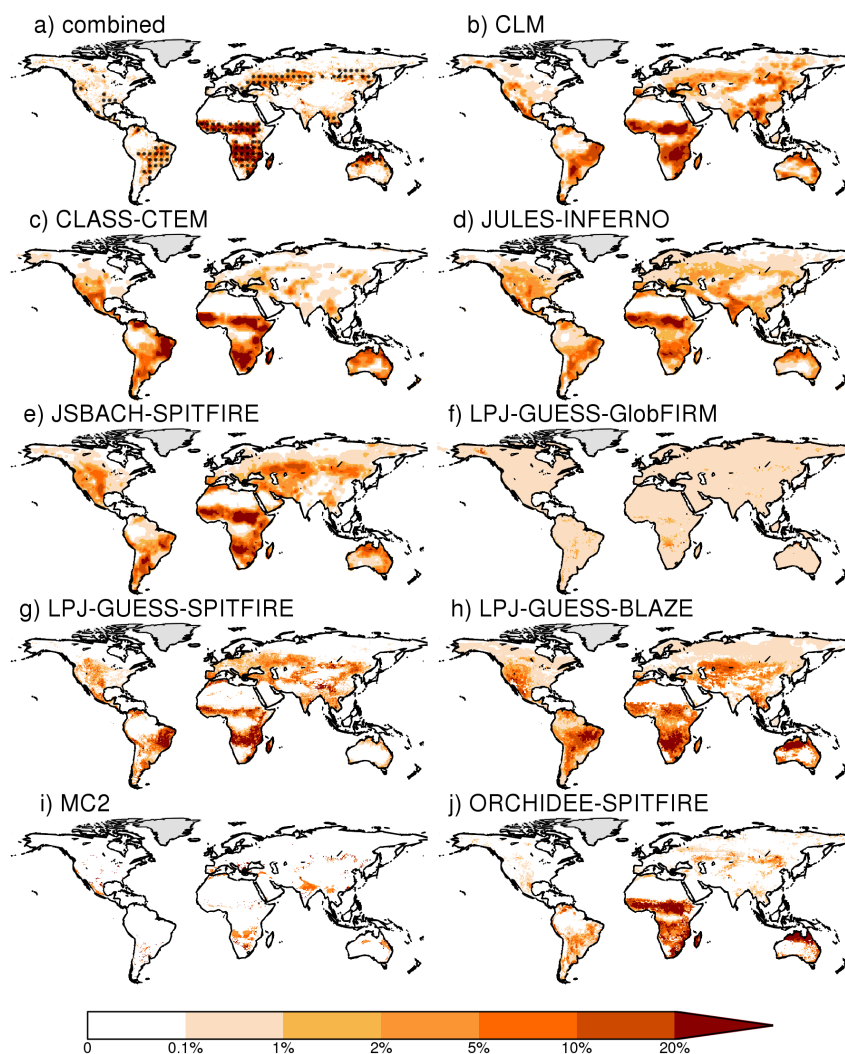


resampled 1000 times without replacement to the observations (Table 3). A detailed description of the benchmarking metrics is given in the Supplementary Information S2.



200 **Figure 1:** Reference datasets, the mean of all models, and the % of models for which the estimate falls within 50-200%  
 of the (mean) reference data are presented for a set of fire relevant variables. Results for the following variables are  
 given: a) fraction burnt area; b) seasonal timing of burnt area (as measured by mean phase); c) burnt area season length  
 (as measured by seasonal concentration); d) fire C emissions ( $\text{g C m}^{-2} \text{yr}^{-1}$ ); e) vegetation carbon ( $\text{Mg/ha}$ ); and f) Leaf  
 205 Area Index (LAI) ( $\text{m}^2/\text{m}^2$ ). Stippling in the 2nd column indicates where variance between models is less than the FireMIP  
 model ensemble mean. Purple in the 3rd column indicates cell where the majority of the FireMIP models produce poor  
 simulations of the variable, while green areas indicate that the majority of the FireMIP models perform well for that  
 aspect of the fire regime.





210 **Figure 2: Simulated versus observed burnt fraction in the present day (2002-2012), where “combined” indicates the mean of the different burnt area datasets considered. Stippling indicates where variance between burnt area datasets is less than the observed ensemble mean.**

### 3 Results

#### 3.1 Modern day model performance: burnt area and fire emissions

215 The simulated modern (2002-2012) total global annual burnt area is between 39 and 536 Mha (Table 2). Most of the FireMIP models are within the range of the remotely sensed observed burnt area (354 to 468 Mha a<sup>-1</sup>). With the exception of MC2 and LPJ-GUESS-GlobFIRM, the models realistically capture the spatial patterns in burnt area (Figures 1 & 2) and perform better than either of the null models irrespective of the reference burnt area dataset (Table 3). CLM (NME: 0.63-0.80) and ORCHIDEE-SPITFIRE (0.70-0.73) are the best performing models.

220 All the FireMIP models correctly simulate most burnt area in the tropics (24-466 Mha a<sup>-1</sup>) compared to observed



values in the range 312-426 Mha a<sup>-1</sup> (Table 2). The simulated contribution of tropical fires to global burnt area is in the range of 56% to 92%, with all models except ORCHIDEE-SPITFIRE simulating a lower fraction than observed (89-93%). This follows from FireMIP models tending to underestimate burnt area in Africa and Australia, although burnt area in South American savannas is usually overestimated (Table 2). All of the FireMIP models, except LPJ-GUESS-GlobFIRM, capture a belt of high burnt area in central Eurasia. However, the models overestimate burnt area across the extratropics on average by 180% to 304%, depending on the reference burnt area dataset. This overestimation largely reflects the fact that the simulated burnt area over the Mediterranean basin and western USA is too large (Table 2, Figure 2).

The FireMIP models that include a sub-annual time-step for fire calculations (CLM, CLASS-CTEM, JULES-INFERNO, JSBACH-SPITFIRE, LPJ-GUESS-SPITFIRE, ORCHIDEE-SPITFIRE) generally reproduce the seasonality of burnt area (Figure 3), particularly in the tropics. The models capture the timing of the peak fire season reasonably well, with all of the models performing better than both null models for seasonal phase in burnt area (Table 3). However, all of the FireMIP models perform worse than both null models for seasonal concentration of burnt area, independent of the reference burnt area dataset. The observations show a unimodal pattern in burnt area in the tropics, peaking between November through February in the northern tropics and between June through October in the southern tropics (Figure 3). The models also show a unimodal pattern in both regions. However, all the FireMIP models except ORCHIDEE-SPITFIRE show a ~2-month delay in peak burnt area in the northern tropics, and the period with high burnt area is also less concentrated than observed. Some models (ORCHIDEE-SPITFIRE, LPJ-GUESS-SPITFIRE) estimate peak burnt area ~1-2 months too early in the southern tropics, while others simulate a peak ~1 month too late (JULES-INFERNO, CLM, CLASS-CTEM) or have a less concentrated peak (JSBACH-SPITFIRE, JULES-INFERNO) than observed. The seasonality of burnt area in the northern extratropics shows a peak in spring and a second peak in summer. Only CLM reproduces this double peak, while all of the other FireMIP models show a single summer peak. Most of the models simulate the timing of the summer peak well. The only exception is LPJ-GUESS-SPITFIRE, which simulates the peak ~2-3 months too late. The observations show no clear seasonal pattern in burnt area over the southern extratropics, although the most prominent peak occurs in December and January. All the FireMIP models, except LPJ-GUESS-SPITFIRE, reproduce this mid-summer peak. LPJ-GUESS-SPITFIRE shows little seasonality in burnt area in this region.

The FireMIP models have problems representing IAV in global burnt area, with some models (CLASS-CTEM, MC2) worse than the random model and most models performing worse than the mean for most of the target data sets (Table 3). However, there is considerable uncertainty in the observed IAV in burnt area (Figure 4), and the scores are therefore dependent on the reference dataset considered, with generally worse scores for FireCCI5.1 and GFED4s compared to the other datasets. Observational uncertainty is most probably underestimated as the burnt area products are not independent, since they all rely on MODIS satellite imagery. Despite the failure to reproduce IAV in general, most of the models show higher burnt area in the early 2000s and a low in 2009-2010 after which burnt area increased again (Figure 4).

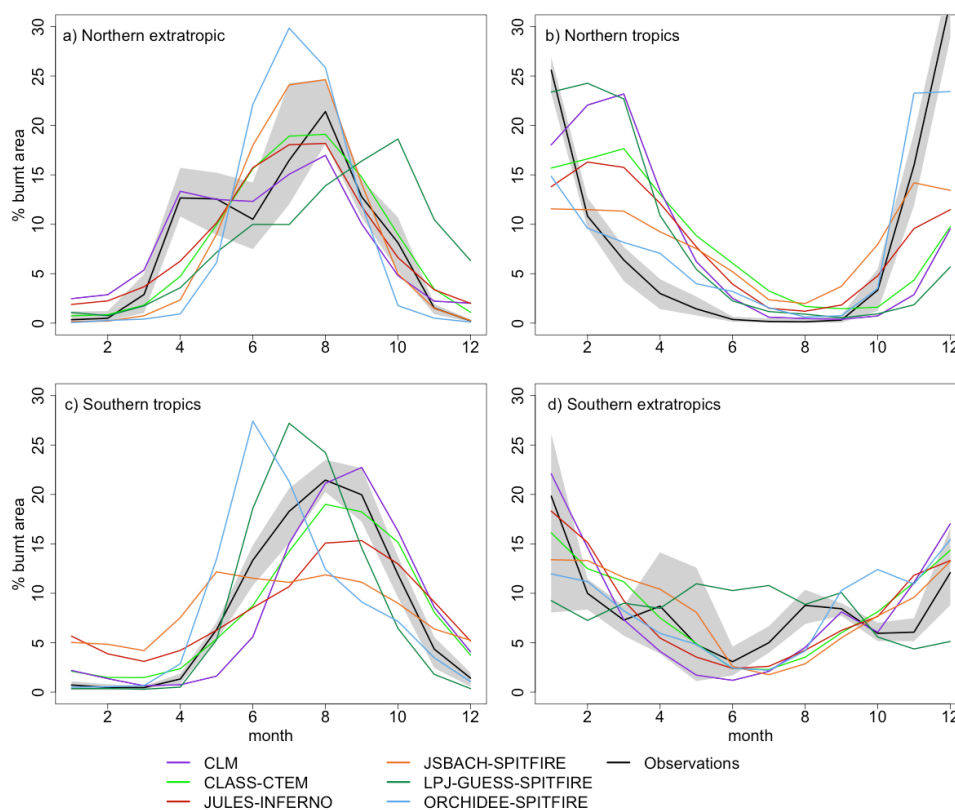
The spatial patterns in simulated fire-related carbon emissions are in line with the reference data, with most FireMIP models except LPJ-GUESS-GlobFIRM, MC2 and LPJ-GUESS-SPITFIRE performing better than the mean model. CLM, JULES-INFERNO and JSBACH-SPITFIRE are the best performing models with NME scores < 0.8. Seasonality in fire emissions mimics the results for burnt area with good scores for seasonal phase, but all models perform worse than the mean null model for seasonal concentration. CLM is the only FireMIP model to explicitly include peatland, cropland and deforestation fires, which contribute 3%, 3% and 20% respectively of the





global total emissions annually (van der Werf et al., 2010), but it nevertheless does not perform better than JULES-INFERNO and JSBACH-SPITFIRE in representing the spatial pattern of fire carbon emissions.

Only three models (JSBACH-SPITFIRE, LPJ-GUESS-SPITFIRE, ORCHIDEE-SPITFIRE) provided information about simulated numbers and size of individual fires. All three models performed better than the mean null model in representing the spatial pattern in number of fires but worse than the mean model for fire size (Table 3). While the spatial pattern in simulated fire number is in agreement with observations over large parts of the globe, models tend to overestimate fire numbers in dryland areas such as Mexico and the Mediterranean basin (Figure 5). None of the three models simulate cropland fires and so they do not capture the high number of cropland fires (Hall et al., 2016) in central Eurasia (Table 2). Models simulate smaller fires than observed in areas where burnt area is large and where models tend to underestimate burnt area, especially in the African savanna regions (Figure 5).



275 **Figure 3: Simulated and observed seasonality (2002-2012) of burnt area (% of annual burnt area per month) for a) northern extratropics ( $> 30^{\circ}\text{N}$ ), b) northern tropics ( $0-30^{\circ}\text{N}$ ), c) southern tropics ( $0-30^{\circ}\text{S}$ ) and d) southern extratropics ( $> 30^{\circ}\text{S}$ ). The mean of all the remotely sensed burnt area datasets is shown as a black line, with the minimum and maximum range shown in light grey.**

280



### 3.2. Present day model performance: Vegetation properties

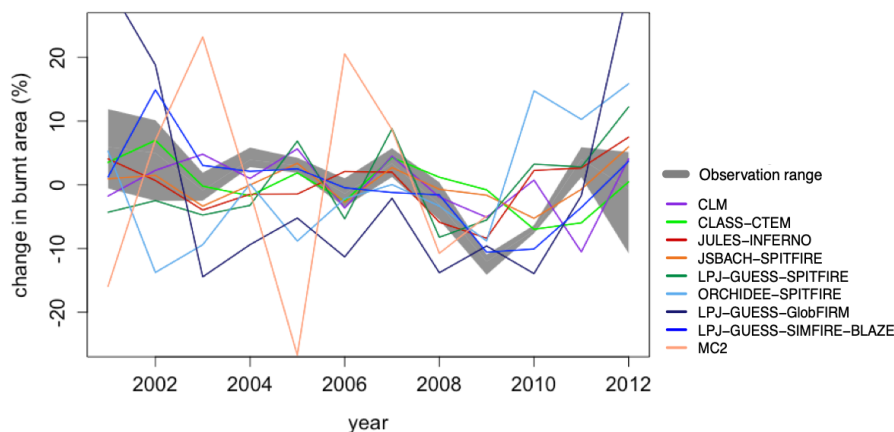
285 Fire spread and hence burnt area is strongly influenced by fuel availability, which in turn is affected by  
vegetation primary production and biomass. Simulated spatial patterns of GPP compare well with estimates of  
GPP upscaled from Fluxnet data (Jung et al., 2017), with scores (0.39-0.67) considerably better than both null  
models. However, performance against site-based estimates of GPP (Luyssaert et al., 2007) are considerably poorer  
(1.09-1.49) and worse than the mean null model. Only LPJ-GUESS-SPITFIRE, LPJ-GUESS-SIMFIRE-BLAZE  
and ORCHIDEE-SPITFIRE perform better than the random null model. There is no clear relationship between  
290 model scores for the two datasets: models performing better when compared to the Jung dataset do not necessarily  
show a higher score when compared to the Luyssaert GPP dataset. The two GPP datasets are very different: The  
upscaled FLUXNET dataset is a modelled product but has global coverage (see Supplementary Information S1)  
while the Luyssaert dataset has local measurements but only at a limited number of sites, largely concentrated  
across the northern extratropics. Thus, the better match between the FireMIP models and the upscaled FLUXNET  
295 dataset may reflect the broader spatial coverage or the fact that climate and landcover data are used for upscaling.

Only the upscaled Fluxnet data provides monthly data and can thus be used to assess GPP seasonality. The  
FireMIP models are able to represent the seasonal peak timing in GPP, with all models performing better than the  
mean and random null models. However, models have difficulty in representing the length of the growing season,  
with the scores for seasonal concentration in GPP (1.08-1.23) above the mean null model but below the random  
300 null model for all FireMIP models.

Model performance is better for site-level NPP than site-level GPP. All of the FireMIP models perform better  
than the mean null model, independent of the choice of reference data set (Table 3), except for CLASS-CTEM  
against the Luyssaert data set. JULES-INFERNNO, JSBACH-SPITFIRE and MC2 are the best-performing models.

305 The FireMIP models generally capture the spatial pattern in LAI, with all models performing better than the  
mean null model (0.44-0.81), independent of the reference dataset considered. JULES-INFERNNO has the best  
score for both reference datasets. Although the overall global pattern in LAI is well represented in all the FireMIP  
models, they have more trouble representing LAI in agricultural areas such as central USA or areas with low LAI  
such as drylands and mountain areas (Figure 1).

310 The FireMIP models perform well in representing the spatial pattern carbon in vegetation (Table 3). All nine  
models perform better than the mean null model, independent of reference dataset, with ORCHIDEE-SPITFIRE  
having the best scores. Generally, the models are able to simulate carbon in tropical vegetation and the forested  
regions in the temperate and boreal region reasonably well, but struggle across most dryland systems (Figure 1).



315 **Figure 4: The range in inter-annual variability in burnt area for the years 2001-2012 for all models and burnt area datasets which span the entire time period (GFED4, GFED4s, MCD45, FireCCI51). Results from the individual FireMIP models, as well as the observational minimum-maximum values, are plotted.**

### 3.3 Overall assessment

320 There is no model that outperforms other models across the full range of fire and vegetation benchmarks examined here. Model structure does not explain the large differences in model performance. Process-based fire models (see table 1) appear to be slightly better able to represent the spatial pattern in burnt area than empirical models (mean score 0.87 and 0.94 respectively), but this difference is largely the result of including GlobFIRM in the empirical model ensemble; removing this model results in a mean score of 0.87 for these models. The inter-model spread in scores within each group is much larger than the difference between the two types of model. Only  
325 one empirical model simulates fire seasonality, but this model performs worse than each of the process-based models, independent of reference dataset considered. There is no difference in the performance of process-based and empirical models with respect to IAV in burnt area, seasonal phase in burnt area or fire emissions.

The FireMIP simulations include three models in which versions of the same process-based fire module (SPITFIRE) are coupled to different vegetation models. These three models produce a wide range of benchmarking  
330 scores for burnt area, with mean benchmarking scores of 0.79, 0.85 and 0.72 for JSBACH, LPJ-GUESS and ORCHIDEE respectively. There are also large differences between these models in terms of other aspects of the fire regime (Table 3). As there are only moderate differences between the different SPITFIRE implementations (Rabin et al., 2017), this suggests that the overall difference between the models reflect feedbacks between the fire and vegetation modules.

335 Models using prescribed vegetation biogeography (CLM, CLASS-CTEM, JSBACH-SPITFIRE, ORCHIDEE-SPITFIRE) represent the spatial pattern of burnt area better than models with dynamic vegetation (JULES-INFERNO, LPJ-GUESS-SPITFIRE, LPJ-GUESS-GlobFIRM, LPJ-GUESS-SIMFIRE-BLAZE, MC2), with respective mean benchmarking scores across all burnt area data sets of 0.79 and 0.97. This difference is still present even when LPJ-GUESS-GlobFIRM and MC2 are not included (0.90). It seems likely that models using prescribed  
340 vegetation biogeography have a better representation of fuel loads and flammability. This can also partially be seen



in the positive relationship between the benchmarking scores of vegetation carbon and burnt area spatial patterns for at least the GFED4, FireCCI4.0 and FireCCI5.1 burnt area reference datasets (mean  $R^2 = 0.31$ , range 0.19-0.38). Areas where the FireMIP models represent vegetation carbon poorly coincide with some of the regions where models have trouble representing the spatial pattern of burnt area such as dryland regions (Figure 1).

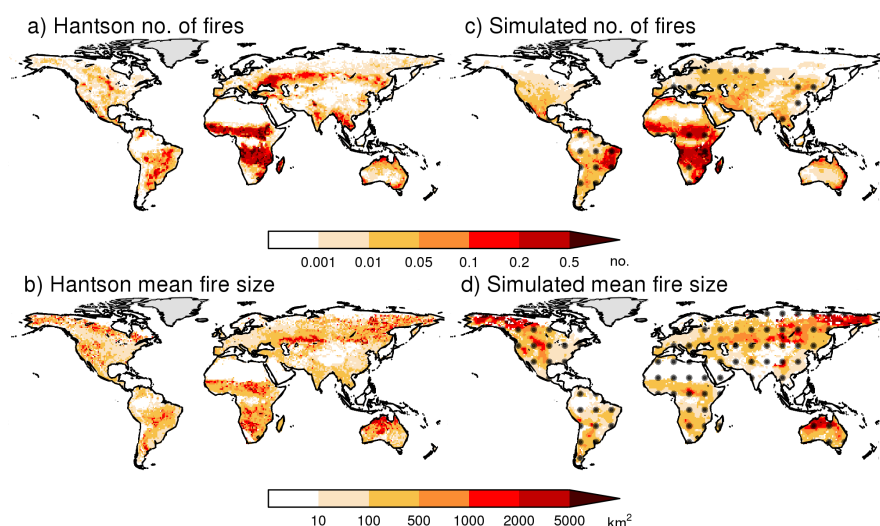
345 Although there is no relationship between GPP/NPP and burnt area benchmarking scores, there is a positive relationship between simulated burnt area scores and the seasonal concentration of GPP ( $R^2 = 0.30-0.84$ ) and, to a lesser extent, the seasonal phase of GPP ( $R^2 = 0.09-0.24$ ). This supports the idea that seasonal vegetation production and senescence, which have an important influence on fuel loads, drive the interactions between vegetation and fire within each model.

350 Fire carbon emission benchmarking scores are strongly related to the burnt area performance ( $R^2 > 0.85$  for GFED4s and MCD45 and  $>0.45$  for FireCCI4.0 and GFED4). This indicates that simulated burnt area is the main driver of fire emissions, overriding spatial patterns in fuel availability and consumption. However, the benchmarking scores for the spatial pattern in burnt area are better overall than those for fire carbon emissions.

Models that explicitly simulate the impact of human suppression on fire growth or burnt area (CLM, CLASS-CTEM, JSBACH-SPITFIRE, LPJ-GUESS-SIMFIRE-BLAZE) are better at representing the spatial pattern in burnt area compared to models which do not include this effect (0.85 and 0.93 respectively). In the case of the three process-based models (CLM, CLASS-CTEM, JSBACH-SPITFIRE) this is most probably because the spatial pattern in fire size is better represented (Table 3).

355 CLM is the only model that incorporates cropland fires (Table 1) and it is also the only model which captures the spring peak in burnt area in the northern extratropics associated with crop fires (e.g. Le Page et al., 2010; Magi et al., 2012, Hall et al., 2016). This might also contribute to the good overall score of CLM for spatial pattern of burnt area.

360



365 **Figure 5: Reference datasets and mean of three models for number of fires and mean fire size. Model output is adapted so that mean and variance coincide with observations as the total values are not directly comparable (See Supplementary Information S1). Stippling indicates where variance between models is less than the model ensemble mean.**



#### 4 Discussion and future model development

There are large differences in the total burnt area between the FireMIP models, with two models (LPJ-GUESS-  
370 GlobFIRM and MC2) falling well outside the observed range in burnt area for the recent period. In the case of  
LPJ-GUESS-GlobFIRM, this is because GlobFIRM was developed before global burnt area products were  
available, resulting in a general poor performance (Kloster and Lasslop, 2017), in combination with the fact that  
structural changes were made to the vegetation model without a commensurate development of the fire module. In  
the case of MC2, this probably reflects the fact that MC2 was developed for regional applications but was applied  
375 globally here without any refinement of the fire model. The other FireMIP models used the burned area datasets  
to develop and tune their models. They therefore capture the global spatial patterns of burnt area reasonably well,  
although no model simulates the very high burnt area in Africa and Australia causing a general underestimation of  
burnt area in tropical regions and overestimation in extratropical regions. The analysis of a limited number of  
models suggests that process-based fire models do not simulate the spatial patterns in fire size well (Table 3). In  
380 particular they fail to represent fire size in tropical savannas (Figure 5), most probably because they assume a fixed  
maximum fire duration of less than one day (Hantson et al., 2016) while savanna fires are often very long-lived  
(e.g. Andela et al., 2019). However, models that include a human limitation on fire growth represent the global  
spatial pattern in burnt area and fire size better. These results indicate that process-based fire models can be  
improved by a better representation of fire duration. The recently generated Global Fire Atlas (Andela et al., 2019)  
385 includes aspects of the fire behaviour (e.g., fire spread rate and duration), which offer new opportunities to examine  
and parameterize fire burning processes simulated by these models.

Inter-model differences in burnt area are related to vegetation production and carbon stocks. Furthermore, we  
find that models which are better at representing the seasonality of vegetation production are also better at  
representing the spatial pattern in burnt area. This indicates that seasonal fuel build-up and senescence is an  
390 important driver of global burnt area. These results are consistent with the analysis of emergent relationships in  
FireMIP models, which shows the need to improve processes related to plant production and biomass allocation  
to improve model performance in simulating burnt area (Forkel et al., 2019a). While there are spatially explicit  
global estimates regarding carbon stocks in live vegetation, there is limited information about carbon stocks of  
different fuel types and how these change between seasons and over time (van Leeuwen et al., 2014; Pettinari &  
395 Chuvieco, 2016). The lack of high-quality fuel availability data currently limits our ability to constrain simulated  
fuel loads.

The FireMIP models generally do not simulate the timing of peak fire occurrence accurately and tend to  
simulate a fire season longer than observed. This might be related to the representation of seasonality in vegetation  
production and fuel build up. However, human activities can also change the timing of fire occurrence (e.g. Le  
400 Page et al., 2010; Rabin et al., 2015), and so an improved representation of the human influence on fire occurrence  
and timing could also help to improve the simulated fire seasonality. The importance of the anthropogenic impact  
on fire seasonality is especially clear in the northern extratropics (e.g. Le Page et al., 2010; Magi et al., 2012),  
where the only model that explicitly includes crop fires (CLM) is also the only model that shows the bimodal  
seasonality.

405 Global inter-annual variability in burnt area is largely driven by drought episodes in high biomass regions and  
fuel buildup after periods of increased rainfall in dryland areas (e.g. Chen et al., 2017). Previous analysis has shown  
that the FireMIP models are relatively good at representing emergent climate-fire relationships (Forkel et al.,  
2019a); hence it seems plausible that fuel buildup and its effect on subsequent burnt area is not well represented



410 in the models and that this is the reason for the poor simulation of IAV in burnt area. This is in line with our  
findings and the findings of Forkel et al. (2019a) that fire models are not sensitive enough to previous previous-  
season vegetation productivity.

415 The spread in simulated global total fire emissions is even larger than for burnt area, but fire emissions largely  
follow the same spatial and temporal patterns as burnt area (Figure 1, table 3). However, the benchmark scores for  
emissions are worse than those for burnt area. This reflects the fact that emissions are the product of both errors in  
420 simulated vegetation and burnt area. Furthermore, spatial and temporal uncertainties in the completeness of  
biomass combustion will affect the emissions. While improvements to vegetation and fuel loads are likely to  
produce more reliable estimates of emissions, an improved representation of the drivers of combustion  
completeness in models will also be required for more accurate fire emission estimates. Only one of the FireMIP  
models (CLM) includes cropland, peatland, and deforestation fire explicitly, albeit in a rather simple way. Our  
425 analyses suggest that this does not produce an improvement in the simulation of either the spatial pattern or timing  
of carbon emissions. However, given that together these fires represent a substantial proportion of annual carbon  
emissions, a focus on developing and testing robust parameterisations for these largely anthropogenic fires could  
also help to provide more accurate fire emission estimates.

425





430 *Competing interests.* The authors declare no competing interest

*Author contribution.* SH and DK analysed the model results; SH, DB, MF, GL, FL, SM, JRM provided global fire-vegetation model outputs; SH, DK, SPH and AA wrote the manuscript with input from all authors.

435 *Code and data availability.* The benchmarking code is archived  
https://zenodo.org/record/3525235#.XdcBzC2ZOcZ (https://doi.org/10.5281/zenodo.3525235). The FireMIP  
model output is archived at https://zenodo.org/record/3555562#.Xell3C2ZOcY (DOI:10.5281/zenodo.3551041).  
Data availability for each reference dataset is provided in the table below:

Variable	Dataset	data access
Burnt area	GFED4	https://www.globalfiredata.org/data.html
	GFED4S	https://www.globalfiredata.org/data.html
	MCD45	Upon request to the author
	FireCCI40	https://geogra.uah.es/fire_cci/
	FireCCI151	https://geogra.uah.es/fire_cci/
Fire emissions	GFAS	https://apps.ecmwf.int/datasets/data/cams-gfas/
Fire size & number	Hantson	https://zenodo.org/record/3564818#.Xelidi2ZOcY
GPP	Luysaert	Upon request to the author
NPP	Jung	https://www.bgc-jena.mpg.de/geodb/projects/Home.php
	Michaletz	https://onlinelibrary.wiley.com/action/downloadSupplement?doi=10.1111%2Fgeb.12685&file=geb12685-sup-0002-supinfo2.xlsx
LAI	Luysaert	Upon request to the author
	EMDI	http://gaim.unh.edu/Structure/Intercomparison/EMDI/validationdata2/
	MCD15	http://doi.org/10.5067/MODIS/MCD15A2H.006
Carbon in vegetation	AVHRR	https://www.ncei.noaa.gov/data/avhrr-land-leaf-area-index-and-fapar/access/
	Avitabile	http://lucid.wur.nl/datasets/high-carbon-ecosystems
	Carvalhois	Upon request to the author

440

*Acknowledgments.* S. Hantson, S. Rabin, and A. Armeth acknowledge support by the EU FP7 projects BACCHUS (grant agreement no. 603445) and LUC4C (grant ag. No. 603542). This work was supported, in part, by the German Federal Ministry of Education and Research (BMBF), through the Helmholtz Association and its research programme ATMO, and the HGF Impulse and Networking fund. S. P. Harrison acknowledges support under the ERC-funded project GC2.0 (Global Change 2.0: Unlocking the past for a clearer future, grant number 694481). D. Kelley was supported by the UK Natural Environment Research Council through The UK Earth System Modelling Project (UKESM, Grant No. NE/N017951/1). GL was funded by the Deutsche Forschungsgemeinschaft (DFG, German Research Foundation – 338130981. F. Li is supported by National Natural Science Foundation of China (41475099 and 41875137).

450



## References

- Abramowitz, G., Herger, N., Gutmann, E., Hammerling, D., Knutti, R., Leduc, M., Lorenz, R., Pincus, R., and Schmidt, G. A.: ESD Reviews: Model dependence in multi-model climate ensembles: weighting, sub-selection and out-of-sample testing, *Earth Syst. Dynam.*, 10, 91-105, 10.5194/esd-10-91-2019, 2019.
- 455 Ahlström, A., Xia, J., Arneeth, A., Luo, Y., and Smith, B.: Importance of vegetation dynamics for future terrestrial carbon cycling, *Environmental Research Letters*, 10, 054019, 2015.
- Allen, C. D., Breshears, D. D., and McDowell, N. G.: On underestimation of global vulnerability to tree mortality and forest die-off from hotter drought in the Anthropocene, *Ecosphere*, 6, 1-55, 2015.
- 460 Alonso-Canas, I., and Chuvieco, E.: Global burned area mapping from ENVISAT-MERIS and MODIS active fire data, *Remote sensing of environment*, 163, 140-152, <http://dx.doi.org/10.1016/j.rse.2015.03.011>, 2015.
- Andela, N., Morton, D. C., Giglio, L., Chen, Y., van der Werf, G. R., Kasibhatla, P. S., DeFries, R. S., Collatz, G. J., Hantson, S., Kloster, S., Bachelet, D., Forrest, M., Lasslop, G., Li, F., Mangeon, S., Melton, J. R., Yue, C., and Randerson, J. T.: A human-driven decline in global burned area, *Science*, 356, 1356-1362, 10.1126/science.aal4108, 2017.
- 465 Andela, N., Morton, D. C., Giglio, L., Paugam, R., Chen, Y., Hantson, S., van der Werf, G. R., and Randerson, J. T.: The Global Fire Atlas of individual fire size, duration, speed and direction, *Earth Syst. Sci. Data*, 11, 529-552, 10.5194/essd-11-529-2019, 2019.
- Archibald, S., Lehmann, C. E. R., Gómez-Dans, J. L., and Bradstock, R. A.: Defining pyromes and global syndromes of fire regimes, *Proceedings of the National Academy of Sciences*, 110, 6442-6447, 10.1073/pnas.1211466110, 2013.
- 470 Arora, V. K., and Melton, J. R.: Reduction in global area burned and wildfire emissions since 1930s enhances carbon uptake by land, *Nature Communications*, 9, 1326, 10.1038/s41467-018-03838-0, 2018.
- Avitabile, V., Herold, M., Heuvelink, G. B. M., Lewis, S. L., Phillips, O. L., Asner, G. P., Armston, J., Ashton, P. S., Banin, L., Bayol, N., Berry, N. J., Boeckx, P., de Jong, B. H. J., DeVries, B., Girardin, C. A. J., Kearsley, E., Lindsell, J. A., Lopez-Gonzalez, G., Lucas, R., Malhi, Y., Morel, A., Mitchard, E. T. A., Nagy, L., Qie, L., Quinones, M. J., Ryan, C. M., Ferry, S. J. W., Sunderland, T., Laurin, G. V., Gatti, R. C., Valentini, R., Verbeeck, H., Wijaya, A., and Willcock, S.: An integrated pan-tropical biomass map using multiple reference datasets, *Global Change Biology*, 22, 1406-1420, 10.1111/gcb.13139, 2016.
- 480 Baccini, A., Goetz, S. J., Walker, W. S., Laporte, N. T., Sun, M., Sulla-Menashe, D., Hackler, J., Beck, P. S. A., Dubayah, R., Friedl, M. A., Samanta, S., and Houghton, R. A.: Estimated carbon dioxide emissions from tropical deforestation improved by carbon-density maps, *Nature Clim. Change*, 2, 182-185, 2012.
- Bachelet, D., Ferschweiler, K., Sheehan, T. J., Sleeter, B. M., and Zhu, Z.: Projected carbon stocks in the conterminous USA with land use and variable fire regimes, *Global Change Biology*, 21, 4548-4560, 2015.
- 485 Bond, W. J., Woodward, F. I., and Midgley, G. F.: The global distribution of ecosystems in a world without fire, *New Phytologist*, 165, 525-538, 2005.
- Bowman, D. M. J. S., Balch, J. K., Artaxo, P., Bond, W. J., Carlson, J. M., Cochrane, M. A., D'Antonio, C. M., DeFries, R. S., Doyle, J. C., Harrison, S. P., Johnston, F. H., Keeley, J. E., Krawchuk, M. A., Kull, C. A., Marston, J. B., Moritz, M. A., Prentice, I. C., Roos, C. I., Scott, A. C., Swetnam, T. W., van der Werf, G. R., and Pyne, S. J.: Fire in the Earth System, *Science*, 324, 481-484, 10.1126/science.1163886, 2009.
- 490



- Bowman, D. M. J. S., Perry, G. L. W., Higgins, S. I., Johnson, C. N., Fuhlendorf, S. D., and Murphy, B. P.: Pyrodiversity is the coupling of biodiversity and fire regimes in food webs, *Philosophical Transactions of the Royal Society of London B: Biological Sciences*, 371, 10.1098/rstb.2015.0169, 2016.
- Carvalhais, N., Forkel, M., Khomik, M., Bellarby, J., Jung, M., Migliavacca, M., u, M., Saatchi, S., Santoro, M.,  
495 Thurner, M., Weber, U., Ahrens, B., Beer, C., Cescatti, A., Randerson, J. T., and Reichstein, M.: Global covariation of carbon turnover times with climate in terrestrial ecosystems, *Nature*, 514, 213-217, 10.1038/nature13731 2014.
- Chen, Y., Morton, D. C., Andela, N., van der Werf, G. R., Giglio, L., and Randerson, J. T.: A pan-tropical cascade of fire driven by El Niño/Southern Oscillation, *Nature Climate Change*, 7, 906-911, 10.1038/s41558-017-0014-8, 2017.  
500
- Collier, N., Hoffman, F. M., Lawrence, D. M., Keppel-Aleks, G., Koven, C. D., Riley, W. J., Mu, M., and Randerson, J. T.: The International Land Model Benchmarking (ILAMB) system: design, theory, and implementation, *Journal of Advances in Modeling Earth Systems*, 10, 2731-2754, 2018.
- Collins, M., Knutti, R., Arblaster, J., Dufresne, J.-L., Fichefet, T., Friedlingstein, P., Gao, X., Gutowski, W. J.,  
505 Johns, T., and Krinner, G.: Long-term climate change: projections, commitments and irreversibility, in: *Climate Change 2013-The Physical Science Basis: Contribution of Working Group I to the Fifth Assessment Report of the Intergovernmental Panel on Climate Change*, Cambridge University Press, 1029-1136, 2013.
- Chuvieco, E., Lizundia-Loiola, J., Pettinari, M. L., Ramo, R., Padilla, M., Tansey, K., Mouillot, F., Laurent, P.,  
510 Storm, T., Heil, A., and Plummer, S.: Generation and analysis of a new global burned area product based on MODIS 250&thinsp;m reflectance bands and thermal anomalies, *Earth Syst. Sci. Data*, 10, 2015-2031, 10.5194/essd-10-2015-2018, 2018.
- Claverie, M., Matthews, J. L., Vermote, E. F., and Justice, C. O.: A 30+ Year AVHRR LAI and FAPAR Climate Data Record: Algorithm Description and Validation, *Remote Sensing*, 8, 263, 2016.
- 515 Eyring, V., Bony, S., Meehl, G. A., Senior, C. A., Stevens, B., Stouffer, R. J., and Taylor, K. E.: Overview of the Coupled Model Intercomparison Project Phase 6 (CMIP6) experimental design and organization, *Geosci. Model Dev.*, 9, 1937-1958, 10.5194/gmd-9-1937-2016, 2016.
- Eyring, V., Harris, N. R. P., Rex, M., Shepherd, T. G., Fahey, D. W., Amanatidis, G. T., Austin, J., Chipperfield, M. P., Dameris, M., Forster, P. M. D. F., Gettelman, A., Graf, H. F., Nagashima, T., Newman, P. A.,  
520 Pawson, S., Prather, M. J., Pyle, J. A., Salawitch, R. J., Santer, B. D., and Waugh, D. W.: A Strategy for Process-Oriented Validation of Coupled Chemistry–Climate Models, *Bulletin of the American Meteorological Society*, 86, 1117-1134, 10.1175/bams-86-8-1117, 2005.
- Forkel, M., Andela, N., Harrison, S. P., Lasslop, G., van Marle, M., Chuvieco, E., Dorigo, W., Forrest, M., Hantson, S., Heil, A., Li, F., Melton, J., Sitch, S., Yue, C., and Arneith, A.: Emergent relationships with  
525 respect to burned area in global satellite observations and fire-enabled vegetation models, *Biogeosciences*, 16, 57-76, 10.5194/bg-16-57-2019, 2019.
- Forkel, M., Dorigo, W., Lasslop, G., Chuvieco, E., Hantson, S., Heil, A., Teubner, I., Thonicke, K., and Harrison, S. P.: Recent global and regional trends in burned area and their compensating environmental controls, *Environmental Research Communications*, 1, 051005, 10.1088/2515-7620/ab25d2, 2019.
- 530 French, N. H. F., de Groot, W. J., Jenkins, L. K., Rogers, B. M., Alvarado, E., Amiro, B., de Jong, B., Goetz, S., Hoy, E., Hyer, E., Keane, R., Law, B. E., McKenzie, D., McNulty, S. G., Ottmar, R., Pérez-Salicrup, D.



- R., Randerson, J., Robertson, K. M., and Turetsky, M.: Model comparisons for estimating carbon emissions from North American wildland fire, *Journal of Geophysical Research: Biogeosciences*, 116, G00K05, 10.1029/2010jg001469, 2011.
- 535 Friend, A. D., Lucht, W., Rademacher, T. T., Keribin, R., Betts, R., Cadule, P., Ciais, P., Clark, D. B., Dankers, R., Falloon, P. D., Ito, A., Kahana, R., Kleidon, A., Lomas, M. R., Nishina, K., Ostberg, S., Pavlick, R., Peylin, P., Schaphoff, S., Vuichard, N., Warszawski, L., Wiltshire, A., and Woodward, F. I.: Carbon residence time dominates uncertainty in terrestrial vegetation responses to future climate and atmospheric CO<sub>2</sub>, *Proceedings of the National Academy of Sciences*, 111, 3280-3285, 10.1073/pnas.1222477110, 540 2014.
- Giglio, L., Randerson, J. T., and Werf, G. R.: Analysis of daily, monthly, and annual burned area using the fourth-generation global fire emissions database (GFED4), *Journal of Geophysical Research: Biogeosciences*, 118, 317-328, 2013.
- Giorgi, F., and Mearns, L. O.: Calculation of Average, Uncertainty Range, and Reliability of Regional Climate Changes from AOGCM Simulations via the “Reliability Ensemble Averaging” (REA) Method, *Journal of Climate*, 15, 1141-1158, 10.1175/1520-0442, 2002.
- 545 Hall, J. V., Loboda, T. V., Giglio, L., and McCarty, G. W.: A MODIS-based burned area assessment for Russian croplands: Mapping requirements and challenges, *Remote sensing of environment*, 184, 506-521, <http://dx.doi.org/10.1016/j.rse.2016.07.022>, 2016.
- 550 Hantson, S., Pueyo, S., and Chuvieco, E.: Global fire size distribution is driven by human impact and climate, *Global Ecology and Biogeography*, 24, 77-86, 10.1111/geb.12246, 2015.
- Hantson, S., Arneth, A., Harrison, S. P., Kelley, D. I., Prentice, I. C., Rabin, S. S., Archibald, S., Mouillot, F., Arnold, S. R., Artaxo, P., Bachelet, D., Ciais, P., Forrest, M., Friedlingstein, P., Hickler, T., Kaplan, J. O., Kloster, S., Knorr, W., Lasslop, G., Li, F., Mangeon, S., Melton, J. R., Meyn, A., Sitch, S., Spessa, A., van 555 der Werf, G. R., Voulgarakis, A., and Yue, C.: The status and challenge of global fire modelling, *Biogeosciences*, 13, 3359-3375, 10.5194/bg-13-3359-2016, 2016.
- Held, I. M.: The Gap between Simulation and Understanding in Climate Modeling, *Bulletin of the American Meteorological Society*, 86, 1609-1614, 10.1175/bams-86-11-1609, 2005.
- Hoegh-Guldberg, O., Jacob, D., Taylor, M., Bindi, M., Brown, S., Camilloni, I., Diedhiou, A., Djalante, R., Ebi, 560 K., and Engelbrecht, F.: Impacts of 1.5 °C global warming on natural and human systems, In: *Global Warming of 1.5°C. An IPCC Special Report on the impacts of global warming of 1.5°C above pre-industrial levels and related global greenhouse gas emission pathways, in the context of strengthening the global response to the threat of climate change, sustainable development, and efforts to eradicate poverty* [Masson-Delmotte, V., P. Zhai, W.-O. Pörtner, D. Roberts, J. Skea, 565 P.R. Shukla, A. Pirani, W. Moufouma-Okia, C. Péan, R. Pidcock, S. Connors, J.B.R. Matthews, W. Chen, X. Zhou, M.I.Gomis, E. Lonnoy, T. Maycock, M. Tignor, and T. Waterfield (eds.)], 2019.
- Jung, M., Reichstein, M., Schwalm, C. R., Huntingford, C., Sitch, S., Ahlström, A., Arneth, A., Camps-Valls, G., Ciais, P., Friedlingstein, P., Gans, F., Ichii, K., Jain, A. K., Kato, E., Papale, D., Poulter, B., Raduly, B., Rödenbeck, C., Tramontana, G., Viovy, N., Wang, Y.-P., Weber, U., Zaehle, S., and Zeng, N.: Compensatory water effects link yearly global land CO<sub>2</sub> sink changes to temperature, *Nature*, 541, 516-520, 10.1038/nature20780, 2017.



- 575 Kaiser, J. W., Heil, A., Andreae, M. O., Benedetti, A., Chubarova, N., Jones, L., Morcrette, J. J., Razinger, M.,  
Schultz, M. G., Suttie, M., and van der Werf, G. R.: Biomass burning emissions estimated with a global  
fire assimilation system based on observed fire radiative power, *Biogeosciences*, 9, 527-554, 10.5194/bg-  
9-527-2012, 2012.
- Kelley, D., Prentice, I. C., Harrison, S., Wang, H., Simard, M., Fisher, J., and Willis, K.: A comprehensive  
benchmarking system for evaluating global vegetation models, *Biogeosciences*, 10, 3313-3340, 2013.
- 580 Kirtman, B., Power, S., Adedoyin, A., Boer, G., Bojariu, R., Camilloni, I., Doblus-Reyes, F., Fiore, A., Kimoto,  
M., and Meehl, G.: Near-term climate change: projections and predictability, In: *Climate Change 2013:  
The Physical Science Basis. Contribution of Working Group I to the Fifth Assessment Report of  
the Intergovernmental Panel on Climate Change* [Stocker, T.F., D. Qin, G.-K. Plattner, M.  
Tignor, S.K. Allen, J. Boschung, A. Nauels, W. Xia, V. Bex and P.M. Midgley (eds.)].  
Cambridge University Press, Cambridge, United Kingdom and New York, NY, USA, 2013.
- 585 Kloster, S., and Lasslop, G.: Historical and future fire occurrence (1850 to 2100) simulated in CMIP5 Earth System  
Models, *Global and Planetary Change*, 150, 58-69, <http://doi.org/10.1016/j.gloplacha.2016.12.017>, 2017.
- Knorr, W., Jiang, L., and Arneth, A.: Climate, CO<sub>2</sub> and human population impacts on global wildfire emissions,  
*Biogeosciences*, 13, 267-282, 10.5194/bg-13-267-2016, 2016.
- Knutti, R.: The end of model democracy?, *Climatic Change*, 102, 395-404, 10.1007/s10584-010-9800-2, 2010.
- 590 Lasslop, G., Coppola, A. I., Voulgarakis, A., Yue, C., and Veraverbeke, S.: Influence of Fire on the Carbon Cycle  
and Climate, *Current Climate Change Reports*, 5, 112-123, 10.1007/s40641-019-00128-9, 2019.
- Lasslop, G., Thonicke, K., and Kloster, S.: SPITFIRE within the MPI Earth system model: Model development  
and evaluation, *Journal of Advances in Modeling Earth Systems*, 6, 740-755, 10.1002/2013ms000284,  
2014.
- 595 Le Page, Y., Oom, D., Silva, J. M. N., Jönsson, P., and Pereira, J. M. C.: Seasonality of vegetation fires as modified  
by human action: observing the deviation from eco-climatic fire regimes, *Global Ecology and  
Biogeography*, 19, 575-588, 10.1111/j.1466-8238.2010.00525.x, 2010.
- Lehsten, V., Tansey, K., Balzter, H., Thonicke, K., Spessa, A., Weber, U., Smith, B., and Arneth, A.: Estimating  
carbon emissions from African wildfires, *Biogeosciences*, 6, 349-360, 10.5194/bg-6-349-2009, 2009.
- 600 Lelieveld, J., Evans, J. S., Fnais, M., Giannadaki, D., and Pozzer, A.: The contribution of outdoor air pollution  
sources to premature mortality on a global scale, *Nature*, 525, 367-371, 10.1038/nature15371, 2015.
- Li, F., Levis, S., and Ward, D.: Quantifying the role of fire in the Earth system—Part 1: Improved global fire  
modeling in the Community Earth System Model (CESM1), *Biogeosciences*, 10, 2293-2314, 2013.
- 605 Li, F., Val Martin, M., Hantson, S., Andreae, M. O., Arneth, A., Lasslop, G., Yue, C., Bachelet, D., Forrest, M.,  
Kaiser, J. W., Kluzek, E., Liu, X., Melton, J. R., Ward, D. S., Darmenov, A., Hickler, T., Ichoku, C., Magi,  
B. I., Sitch, S., van der Werf, G. R., and Wiedinmyer, C.: Historical (1700-2012) Global Multi-model  
Estimates of the Fire Emissions from the Fire Modeling Intercomparison Project (FireMIP), *Atmos. Chem.  
Phys. Discuss.*, 2019, 1-57, 10.5194/acp-2019-37, 2019.
- Luyssaert, S., Inglima, I., Jung, M., Richardson, A. D., Reichsteins, M., Papale, D., Piao, S. L., Schulzes, E. D.,  
610 Wingate, L., Matteucci, G., Aragao, L., Aubinet, M., Beers, C., Bernhoffer, C., Black, K. G., Bonal, D.,  
Bonnefond, J. M., Chambers, J., Ciais, P., Cook, B., Davis, K. J., Dolman, A. J., Gielen, B., Goulden, M.,  
Grace, J., Granier, A., Grelle, A., Griffis, T., Gruenwald, T., Guidolotti, G., Hanson, P. J., Harding, R.,  
Hollinger, D. Y., Hutrya, L. R., Kolar, P., Kruijt, B., Kutsch, W., Lagergren, F., Laurila, T., Law, B. E.,



- 615 Le Maire, G., Lindroth, A., Loustau, D., Malhi, Y., Mateus, J., Migliavacca, M., Misson, L., Montagnani, L., Moncrieff, J., Moors, E., Munger, J. W., Nikinmaa, E., Ollinger, S. V., Pita, G., Rebmann, C., Rouspard, O., Saigusa, N., Sanz, M. J., Seufert, G., Sierra, C., Smith, M. L., Tang, J., Valentini, R., Vesala, T., and Janssens, I. A.: CO<sub>2</sub> balance of boreal, temperate, and tropical forests derived from a global database, *Global Change Biology*, 13, 2509-2537, 10.1111/j.1365-2486.2007.01439.x, 2007.
- 620 Magi, B. I., Rabin, S., Shevliakova, E., and Pacala, S.: Separating agricultural and non-agricultural fire seasonality at regional scales, *Biogeosciences*, 9, 3003-3012, 10.5194/bg-9-3003-2012, 2012.
- Mangeon, S., Voulgarakis, A., Gilham, R., Harper, A., Sitch, S., and Folberth, G.: INFERNO: a fire and emissions scheme for the Met Office's Unified Model, *Geosci. Model Dev. Discuss.*, 2016, 1-21, 10.5194/gmd-2016-32, 2016.
- 625 Melton, J. R., and Arora, V. K.: Competition between plant functional types in the Canadian Terrestrial Ecosystem Model (CTEM) v. 2.0, *Geosci. Model Dev.*, 9, 323-361, 10.5194/gmd-9-323-2016, 2016.
- Michaletz, S. T., Cheng, D., Kerkhoff, A. J., and Enquist, B. J.: Convergence of terrestrial plant production across global climate gradients, *Nature*, 512, 39-43, 10.1038/nature13470, 2014.
- 630 Myneni, R. B., Hoffman, S., Knyazikhin, Y., Privette, J. L., Glassy, J., Tian, Y., Wang, Y., Song, X., Zhang, Y., Smith, G. R., Lotsch, A., Friedl, M., Morisette, J. T., Votava, P., Nemani, R. R., and Running, S. W.: Global products of vegetation leaf area and fraction absorbed PAR from year one of MODIS data, *Remote Sensing of Environment*, 83, 214-231, [https://doi.org/10.1016/S0034-4257\(02\)00074-3](https://doi.org/10.1016/S0034-4257(02)00074-3), 2002.
- Olson, R., Johnson, K., Zheng, D., and Scurlock, J.: Global and regional ecosystem modeling: Databases of model drivers and validation measurements, ORNL Technical Memorandum TM-2001/196. Oak Ridge National Laboratory, Oak Ridge, Tennessee, USA, 2001.
- 635 Parker, W. S.: Ensemble modeling, uncertainty and robust predictions, *Wiley Interdisciplinary Reviews: Climate Change*, 4, 213-223, 10.1002/wcc.220, 2013.
- Pettinari, M. L., and Chuvieco, E.: Generation of a global fuel data set using the Fuel Characteristic Classification System, *Biogeosciences*, 13, 2061-2076, 10.5194/bg-13-2061-2016, 2016.
- 640 Rabin, S. S., Melton, J. R., Lasslop, G., Bachelet, D., Forrest, M., Hantson, S., Kaplan, J. O., Li, F., Mangeon, S., Ward, D. S., Yue, C., Arora, V. K., Hickler, T., Kloster, S., Knorr, W., Nieradzik, L., Spessa, A., Folberth, G. A., Sheehan, T., Voulgarakis, A., Kelley, D. I., Prentice, I. C., Sitch, S., Harrison, S., and Arneth, A.: The Fire Modeling Intercomparison Project (FireMIP), phase 1: experimental and analytical protocols with detailed model descriptions, *Geosci. Model Dev.*, 10, 1175-1197, 10.5194/gmd-10-1175-2017, 2017.
- Randerson, J., Chen, Y., Werf, G., Rogers, B., and Morton, D.: Global burned area and biomass burning emissions from small fires, *Journal of Geophysical Research: Biogeosciences (2005–2012)*, 117, 2012.
- 645 Roteta, E., Bastarrika, A., Padilla, M., Storm, T., and Chuvieco, E.: Development of a Sentinel-2 burned area algorithm: Generation of a small fire database for sub-Saharan Africa, *Remote Sensing of Environment*, 222, 1-17, <https://doi.org/10.1016/j.rse.2018.12.011>, 2019.
- Roy, D. P., Boschetti, L., Justice, C. O., and Ju, J.: The collection 5 MODIS burned area product — Global evaluation by comparison with the MODIS active fire product, *Remote sensing of environment*, 112, 3690-3707, 2008.
- 650 Saatchi, S. S., Harris, N. L., Brown, S., Lefsky, M., Mitchard, E. T. A., Salas, W., Zutta, B. R., Buermann, W., Lewis, S. L., Hagen, S., Petrova, S., White, L., Silman, M., and Morel, A.: Benchmark map of forest carbon





- stocks in tropical regions across three continents, *Proceedings of the National Academy of Sciences*, 108,  
655 9899-9904, 10.1073/pnas.1019576108, 2011.
- Santer, B. D., Taylor, K. E., Gleckler, P. J., Bonfils, C., Barnett, T. P., Pierce, D. W., Wigley, T. M. L., Mears, C.,  
Wentz, F. J., Brüggemann, W., Gillett, N. P., Klein, S. A., Solomon, S., Stott, P. A., and Wehner, M. F.:  
Incorporating model quality information in climate change detection and attribution studies, *Proceedings*  
of the National Academy of Sciences, 106, 14778-14783, 10.1073/pnas.0901736106, 2009.
- 660 Settele, J., Scholes, R., Betts, R., Bunn, S., Leadley, P., Nepstad, D., Overpeck, J. T., and Taboada, M.  
A.: Terrestrial and inland water systems, in: *Climate change 2014: Impacts, adaptation, and*  
*vulnerability. Part a: Global and sectoral aspects. Contribution of working group ii to the fifth*  
*assessment report of the intergovernmental panel on climate change*, edited by: Field, C. B.,  
Barros, V. R., Dokken, D. J., Mach, K. J., Mastrandrea, M. D., Bilir, T. E., Chatterjee, M., Ebi,  
665 K. L., Estrada, W. O., Genova, R. C., Girma, B., Kissel, E. S., Levy, A. N., MacCracken, S.,  
Mastrandrea, P. R., and L.L., W., Cambridge University Press, Cambridge, 271-359, 2014.
- Smith, B., Wårlind, D., Arneth, A., Hickler, T., Leadley, P., Siltberg, J., and Zaehle, S.: Implications of  
incorporating N cycling and N limitations on primary production in an individual-based dynamic  
vegetation model, *Biogeosciences*, 11, 2027-2054, 10.5194/bg-11-2027-2014, 2014.
- 670 Song, X., Li, F., Harrison, S.P., Arneth, A., Forrest, M., Hantson, S., Lasslop, G., Mangeon, S., Melton,  
J.R., Yue, C., Hickler, T., Xu, X. Assessment of vegetation biomass and its 20<sup>th</sup> century changes  
over China based on a combination of multi-model simulations and field observations.  
*Environmental Research Letters*, subm., 2019.
- Taylor, K. E., Stouffer, R. J., and Meehl, G. A.: An overview of CMIP5 and the experiment design, *Bull. Am.*  
675 *Meteorol. Soc.*, 93, DOI:0.1175/BAMS-D-1111-00094.00091, 2012.
- Teckentrup, L., Harrison, S. P., Hantson, S., Heil, A., Melton, J. R., Forrest, M., Li, F., Yue, C., Arneth, A., Hickler,  
T., Sitch, S., and Lasslop, G.: Sensitivity of simulated historical burned area to environmental  
and anthropogenic controls: A comparison of seven fire models, *Biogeosciences Discuss.*, 1-39,  
10.5194/bg-2019-42, accepted, 2019.
- 680 Thurner, M., Beer, C., Santoro, M., Carvalhais, N., Wutzler, T., Schepaschenko, D., Shvidenko, A., Kompter, E.,  
Ahrens, B., Levick, S. R., and Schimmlius, C.: Carbon stock and density of northern boreal and temperate  
forests, *Global Ecology and Biogeography*, 23, 297-310, 10.1111/geb.12125, 2014.
- Tramontana, G., Jung, M., Schwalm, C. R., Ichii, K., Camps-Valls, G., Ráduly, B., Reichstein, M., Arain, M. A.,  
Cescatti, A., Kiely, G., Merbold, L., Serrano-Ortiz, P., Sickert, S., Wolf, S., and Papale, D.: Predicting  
685 carbon dioxide and energy fluxes across global FLUXNET sites with regression algorithms,  
*Biogeosciences*, 13, 4291-4313, 10.5194/bg-13-4291-2016, 2016.
- van der Werf, G. R., Randerson, J. T., Giglio, L., Collatz, G. J., Mu, M., Kasibhatla, P. S., Morton, D. C., DeFries,  
R. S., Jin, Y., and van Leeuwen, T. T.: Global fire emissions and the contribution of deforestation, savanna,  
forest, agricultural, and peat fires (1997-2009), *Atmospheric Chemistry and Physics*, 10, 11707-11735,  
690 DOI 10.5194/acp-10-11707-2010, 2010.
- van Leeuwen, T. T., van der Werf, G. R., Hoffmann, A. A., Detmers, R. G., Rucker, G., French, N. H. F., Archibald,  
S., Carvalho Jr, J. A., Cook, G. D., de Groot, W. J., Hély, C., Kasischke, E. S., Kloster, S., McCarty, J. L.,  
Pettinari, M. L., Savadogo, P., Alvarado, E. C., Boschetti, L., Manuri, S., Meyer, C. P., Siegert, F.,



- 695 Trollope, L. A., and Trollope, W. S. W.: Biomass burning fuel consumption rates: a field measurement database, *Biogeosciences*, 11, 7305-7329, 10.5194/bg-11-7305-2014, 2014.
- Warszawski, L., Friend, A., Ostberg, S., Frieler, K., Lucht, W., Schaphoff, S., Beerling, D., Cadule, P., Ciais, P., Clark, D. B., Kahana, R., Ito, A., Keribin, R., Kleidon, A., Lomas, M., Nishina, K., Pavlick, R., Rademacher, T. T., Buechner, M., Piontek, F., Schewe, J., Serdeczny, O., and Schellnhuber, H. J.: A multi-model analysis of risk of ecosystem shifts under climate change, *Environmental Research Letters*, 8, 044018, 10.1088/1748-9326/8/4/044018, 2013.
- 700 Ward, D. S., Shevliakova, E., Malyshev, S., Lamarque, J. F., and Wittenberg, A. T.: Variability of fire emissions on interannual to multi-decadal timescales in two Earth System models, *Environmental Research Letters*, 11, 125008, 2016.
- Weigel, A. P., Liniger, M. A., and Appenzeller, C.: Can multi-model combination really enhance the prediction skill of probabilistic ensemble forecasts?, *Q J Roy Meteor Soc*, 134, 241-260, 10.1002/qj.210, 2008.
- 705 Wu, M., Knorr, W., Thonicke, K., Schurgers, G., Camia, A., and Arneth, A.: Sensitivity of burned area in Europe to climate change, atmospheric CO<sub>2</sub> levels, and demography: A comparison of two fire-vegetation models, *Journal of Geophysical Research: Biogeosciences*, 120, 2256-2272, 2015.
- 710 Yue, C., Ciais, P., Cadule, P., Thonicke, K., Archibald, S., Poulter, B., Hao, W. M., Hantson, S., Mouillot, F., Friedlingstein, P., Maignan, F., and Viovy, N.: Modelling the role of fires in the terrestrial carbon balance by incorporating SPITFIRE into the global vegetation model ORCHIDEE – Part 1: simulating historical global burned area and fire regimes, *Geosci. Model Dev.*, 7, 2747-2767, 10.5194/gmd-7-2747-2014, 2014.

715



**Table 1: Brief description of the global fire models that ran the FireMIP baseline experiments. Process indicates models which explicitly simulate ignitions and fire spread. A detailed overview can be found in Rabin et al. (2017).**

<i>Model</i>	<i>Dynamic Biogeography</i>	<i>Fire model type</i>	<i>Human suppression of fire spread/ burnt area</i>	<i>Spatial resolution (lon x lat)</i>	<i>Temporal resolution</i>	<i>Reference</i>
CLM	No	Process	Yes	2.5° x 1.9°	Half hourly	Li et al., 2013
CLASS-CTEM	No	Process	Yes	2.8125° x 2.8125°	Daily	Melton and Arora, 2016
JULES-INFERNO	Yes, but without fire feedback	Empirical	No	1.875° x 1.245°	Half hourly	Mangeon et al., 2016
JSBACH-SPTFIRE	No	Process	Yes	1.875° x 1.875°	Daily	Lasslop et al., 2014
LPI-GUESS-SPTFIRE	Yes	Process	No	0.5° x 0.5°	Daily	Lehsten et al., 2009
LPI-GUESS-GlobFIRM	Yes	Empirical	No	0.5° x 0.5°	Annual	Smith et al., 2014
LPI-GUESS-SIMFIRE-BLAZE	Yes	Empirical	Yes	0.5° x 0.5°	Annual	Knorr et al., 2016
MOC2	Yes	Process	No	0.5° x 0.5°	Monthly	Bachelet et al., 2015
ORCHIDEE-SPTFIRE	No	Process	No	0.5° x 0.5°	Daily	Yue et al., 2014



**Table 2:** Simulated and observed burnt area (Mha) for the period 2002-2012 for the globe and for key regions including the northern extratropics (NET, > 30°N), the southern extratropics (SET, < 30°S), the tropics (30°N - 30°S), the savanna regions of Africa (18°W-40°E & 13°N-20°S), the savanna region of South America (42°-68°W & 9°S-25°S), Australian Savanna (120°E-155°E & 11°S-20°S), the agricultural band of central Eurasia (30°E-85°E & 50°N-58°N), the Mediterranean basin (10°W-37°E & 31°N-44°N), and the western USA (100°-125°W & 31°N-43°N). Data availability for FireCCI40 is limited to 2005-2011 and for MC2 to 2002-2009.

	Global	NET	Tropics	SET	S-American savanna	African savanna	Australian savanna	Central Eurasia	Mediterranean basin	western USA
GFED4s	468	39	426	4	18	295	35	8.5	1.3	1.0
GFED4	349	27	319	3	14	218	34	5.2	0.8	0.9
MCD45	348	33	312	4	13	232	25	7.0	2.0	0.9
FireCCI40	345	23	320	2	8	237	25	6.8	1.1	0.8
FireCCI51	387	37	347	3	14	230	38	10.2	1.3	1.1
CLM	454	77	362	15	36	194	15	7.9	9.3	3.4
CLASS-CTEM	536	41	466	28	46	172	20	2.0	4.3	9.5
JULES-INFERNO	343	70	261	12	23	121	20	5.2	11.7	6.1
JSBACH-SPTFIRE	457	114	318	25	21	166	17	15.5	9.5	9.7
LPI-GUESS-GlobFIRM	39	14	24	1	3	7	3	0.6	0.6	0.5
LPI-GUESS-SPTFIRE	393	99	280	14	51	135	2.8	12.5	14.5	6.1
LPI-GUESS-SIMFIRE-BLAZE	482	86	381	15	72	146	27	3.4	7.9	14.9
MC2	97	40	54	3	2	17	2	0.9	5.0	2.2
ORCHIDEE-SPTFIRE	471	16	435	19	13	246	81	2.4	2.4	0.3

720

725

730

735

740

745

750

755



760

**Table 3: Benchmarking scores after removing the influence of differences in the mean and variance for each individual global fire model for key fire and vegetation variables. A lower score is “better”, with a perfect score equal to 0. The full table with all benchmarking scores is presented in Table S1. Dataset information can be found in Supplementary Information S1. LPJ-G = LPJ-GUESS.**

	<i>Dataset</i>	<i>Mean</i>	<i>random</i>	<i>CLM</i>	<i>CLASS-CTEM</i>	<i>JULES INFERNO</i>	<i>JSBACH SPITFIRE</i>	<i>LPJ-G GlobFIRM</i>	<i>LPJ-G SPITFIRE</i>	<i>SIMFIRE -BLAZE</i>	<i>MC2</i>	<i>ORCHIDEE SPITFIRE</i>
<b>Burnt area</b>												
<i>spatial</i>	GFED4s	1	1.07	0.63	0.79	0.72	0.70	1.06	0.94	0.88	1.00	0.72
	GFED4	1	1.14	0.80	0.93	0.85	0.86	1.08	0.98	0.88	1.07	0.71
	MCD45	1	1.16	0.65	0.81	0.72	0.69	1.12	0.93	0.92	1.02	0.70
	FireCCI40	1	1.13	0.77	0.98	0.89	0.92	1.09	0.93	0.97	1.13	0.73
	FireCCI51	1	1.11	0.83	1.01	0.91	0.93	1.11	0.96	0.97	1.23	0.70
<i>seasonal phase</i>	GFED4s	0.56	0.22	0.12	0.12	0.13	0.12		0.31			0.31
	GFED4	0.49	0.47	0.34	0.35	0.41	0.42		0.33			0.31
	MCD45	0.56	0.26	0.12	0.11	0.12	0.12		0.30			0.30
	FireCCI40	0.60	0.12	0.16	0.43	0.17	0.16		0.33			0.32
	FireCCI51	0.55	0.25	0.26	0.28	0.33	0.32		0.32			0.31
<i>seasonal concentration</i>	GFED4s	1	1.36	1.16	1.15	1.24	1.15		1.13			1.22
	GFED4	1	1.35	1.19	1.12	1.25	1.11		1.18			1.19
	MCD45	1	1.36	1.14	1.08	1.26	1.13		1.12			1.20
	FireCCI40	1	1.34	1.31	1.26	1.36	1.25		1.29			1.30
	FireCCI51	1	1.36	1.25	1.22	1.33	1.21		1.20			1.27
<i>IAV</i>	GFED4s	1	1.46	1.17	0.65	1.18	1.09	0.66	1.36	0.76	1.66	1.44
	GFED4	1	1.27	0.98	1.62	1.23	0.89	1.04	1.08	1.00	1.41	1.25
	MCD45	1	1.32	0.93	1.34	1.11	0.84	0.73	0.97	1.27	1.67	1.22
	FireCCI5.1	1	1.42	1.18	1.53	1.24	1.27	1.73	1.27	1.23	1.87	1.12
<b>fire emission</b>												
<i>spatial</i>	GFAS	1	1.08	0.78	0.85	0.73	0.74	1.13	1.03	0.91	1.06	0.86
<i>seasonal phase</i>	GFAS	0.78	0.18	0.16	0.20	0.17	0.15		0.37			0.34
<i>seasonal concentration</i>	GFAS	1	1.36	1.20	1.22	1.30	1.17		1.27			1.25
<i>IAV</i>	GFAS	1	1.36	0.77	1.70	1.28	1.09	1.42	1.42	1.11	1.41	1.49
<b>Fire number</b>												
<i>spatial</i>	Hantson	1	1.19				0.96		0.83			0.76
<b>Fire size</b>												
<i>Spatial</i>	Hantson	1	1.31				1.03		1.22			1.12
<b>GPP</b>												
<i>spatial</i>	Luyssaert	1	1.39	1.49	1.41	1.46	1.39	1.41	1.24	1.37		1.09
<i>spatial</i>	Jung	1	1.30	0.64	0.46	0.39	0.42	0.46	0.67	0.43		0.49
<i>seasonal phase</i>	Jung	0.42	0.65	0.18	0.23	0.19	0.23		0.22			0.22
<i>seasonal concentration</i>	Jung	1	1.65	1.08	1.19	1.14	1.21		1.19			1.09
<b>NPP</b>												
<i>spatial</i>	Michaletz	1	1.39	0.82	0.79	0.77	0.75	0.96	0.86	0.89	0.88	0.99
<i>spatial</i>	Luyssaert	1	1.33	0.90	1.01	0.53	0.76	0.82	0.87	0.79	0.68	0.84
<i>spatial</i>	EMDI	1	1.30	0.91	0.87	0.58	0.66	0.79	0.83	0.81	0.65	0.80
<b>LAI</b>												
<i>spatial</i>	MCD15	1	1.29	0.60	0.53	0.44	0.78	0.70	0.61	0.57	0.63	
<i>spatial</i>	AVHRR	1	1.29	0.81	0.71	0.49	0.65	0.74	0.62	0.61	0.64	
<b>Carbon in vegetation</b>												
<i>spatial</i>	Avitabile	1	1.32	0.69	0.88	0.76	0.78	0.76	0.76	0.74	0.80	0.70
<i>spatial</i>	Carvalhais	1	1.32	0.66	0.66	0.58	0.64	0.62	0.66	0.58	0.67	0.54